Motion Artifact Reduction from Finger Photoplethysmogram Using Discrete Wavelet Transform

Anita Biswas, Monalisa Singha Roy and Rajarshi Gupta

Abstract In this work, discrete wavelet transform was used to remove the effect of motion artifact on the Photoplethysmogram (PPG) signal obtained at fingertip. Clean PPG signal and motion data (one direction) were collected from 40 healthy volunteers at 14-bit resolution using NI 6009 DAQ card, and synthetic noisy signal was generated by addition. The noisy signal was first decomposed into a specific number of levels to obtain different frequency bands. Then, soft thresholding method was used to remove the noisy components. Different wavelet functions (Daubechies, Symlet, Coiflet) and soft thresholding methods ('rigrsure,' 'heursure,' 'sqtwolog,' etc.) were used to denoise the corrupted PPG signal. A comparative study was made between all of these methods by calculating performance measures such as signal-to-noise ratio improvement, mean square error, and percentage noise retention. The mother wavelet 'Db6' and 'rigrsure' soft thresholding method showed the best result.

Keywords Photoplethysmogram · Motion artifact · Discrete wavelet transform Thresholding · Denoising

1 Introduction

During the last two decades, the Photoplethysmography (PPG) technique has become an emerging area of research for its wide application in clinical physiological monitoring [1]. PPG is a simple, noninvasive optoelectronic method to detect the blood volume changes on the peripheral body parts. The PPG sensor detects change in light intensity due to blood volume changes as a result of cardiac systole and diastole

A. Biswas (✉) · M. Singha Roy · R. Gupta
Department of Applied Physics, University of Calcutta, Kolkata, India
e-mail: anitabiswas.biswas8@gmail.com

M. Singha Roy
e-mail: monalisa_sr03@yahoo.co.in

R. Gupta
e-mail: rgaphy@caluniv.ac.in

S. Bhattacharyya et al. (eds.), *Recent Trends in Signal and Image Processing*,
Advances in Intelligent Systems and Computing 727,
https://doi.org/10.1007/978-981-10-8863-6_10

[2, 3] using near red and infrared wavelength light source and detector. It is found that PPG waveform can provide a lot of valuable clinical information such as blood pressure, heart rate, respiratory rate, and cardiac output [4–6].

However, for ubiquitous and real-time measurement system, PPG signals are easily prone to motion artifacts (MA) which could lead to inaccurate interpretation of the PPG waveform. The common sources of errors are ambient light at the photodetector, poor contact of the PPG sensor and the skin, patient's movement, respiration, etc. [7, 8]. The motion artifacts which mix the raw PPG signal that resides in the same frequency range with the actual PPG data (0–2 Hz). In particular, the motion artifact reduction is the most challenging issue. Over the last few years, many researchers focused on the area of motion artifacts removal technique from PPG signal.

The adaptive filtering technique used in real-time application is a well-known method for motion artifacts removal. But it requires an additional sensor to provide reference signal which is the major drawback of this method [9, 10]. AS-LMS adaptive filter eliminates this drawback by generating the reference signal internally from the MA-corrupted PPG itself. Principal Component Analysis (PCA) is a popular signal processing tool that can be effectively used for noise elimination, signal separation, and feature extraction. By selecting suitable number of principal components, the dimension of the actual data can be reduced but also retaining maximum possible information of the actual data [11]. In [12], the frequency characteristics of the PPG signal are analyzed to characterize the clean PPG and motion artifact. It is observed that the raw PPG has fundamental, second and third harmonic structure caused by arterial blood flow and component caused by motion artifact. The raw signal is divided into different groups depending on the relative location of these frequency components. The motion artifact is composed of single frequency component. Another frequency domain analysis method named Empirical Mode Decomposition (EMD), that empirically extracts the oscillatory behavior from the signal and decompose a time series data into a number of intrinsic mode function (IMFs). In [13], Hilbert Hung Transform is used to generate instantaneous frequency for each IMF. The PPG signal is divided into six scales of different frequency bands. According to mean frequency, the scales 1–3 match with clean PPG signal and its harmonics and scales 4–6 correlate with the motion artifacts. An improved algorithm is presented in [14] which combine PCA with the EMD method to generate a smaller group of orthogonal variables. A fewer number of principal components are able to represent the clinical information of the signal, and this number is always less than the number of IMFs. In all of these frequency domain methods, the Fast Fourier Transform (FFT) is used to convert the signal from time domain to frequency domain. Wavelet transform is a powerful tool that has been widely used in ECG signal denoising. However, its application in PPG preprocessing is comparatively fewer [15, 16]. In [16], application of wavelet transform for MA reduction is described. However, the authors only evaluated the systolic peak amplitude variations and spectrum analysis and no detailed study on error parameters was done.

In this work, we used synthetic noisy PPG by imposing three different noise levels and decompose the signal using DWT. The performance of different mother wavelets and different thresholding rules on signal reconstruction quality was also

investigated. Additionally, a detailed study on error parameters was done to evaluate the effectiveness of the proposed method.

2 Methodology

2.1 Data Collection Protocol

The PPG signal was recorded from forty male and female volunteers in the age group 20–45 years. Prior to data collection, they were requested to sit in a relaxed condition. A transmission type PPG sensor was placed on the left hand index finger, kept in stationary condition, while an accelerometer was attached on the right hand index finger. For our application, we considered only horizontal movement of the hand (X-axis). The right hand was moved from elbow at three predefined levels of motion (level, i.e., 10, 15, and 20 cm), each non-periodic. For every subject, data collection was done for 30 s. at 60 Hz using NI6009 DAQ device. The motion data was added with the clean PPG signal in different proportions to generate synthetic noisy signal. The PPG data was stored in calibrated voltage format against sampling time in <*.txt> formatted file.

2.2 Wavelet Denoising Approach

Because the PPG signal is non-stationary in nature, the discrete wavelet transform (DWT) is an appropriate signal processing tool for analyzing the time–amplitude information from a signal. It analyzes the signal at different resolutions by decomposing it into various successive frequency bands. The signal is passed through a series of high-pass filter and low-pass filter.

Since in DWT the signal is a discrete time function, it can be represented as x[n], where n is an integer. The signal is passed through a half band digital low-pass filter with impulse response h[n]. The convolution operation in discrete time is defined as follows:

$$x[n] * h[n] = \sum_{k=-\infty}^{\infty} x[k] \cdot h[n-k] \tag{1}$$

The half band low-pass filter removes all the frequencies that are above half of the highest frequency in the signal.

The denoising algorithm is given below:

a. Decomposition—The input signal was decomposed up to level 5 (to get a frequency level around 1.7 Hz, that of PPG signal) by choosing appropriate wavelet

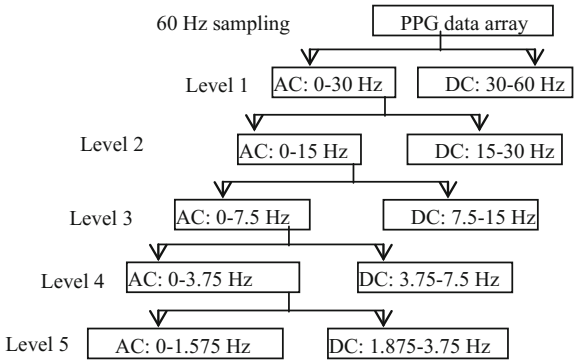

Fig. 1 Wavelet decomposition structure of the PPG data

function using Daubechies6 (Db6) as the basis wavelet. The decomposition structure is shown in Fig. 1.

b. Thresholding—In 'soft' thresholding, the coefficients below a threshold value are set to zero, while the magnitude of others is truncated by the same value. Mathematically, it is expressed as

$$\begin{aligned} \hat{d}_{j,k} &= sign(d_{j,k})|d_{j,k} - t|, \ \ if \ \ |d_{j,k}| > t \\ &= 0, \ \ otherwise \end{aligned} \tag{2}$$

where $d_{j,k}$ represents the kth wavelet coefficient in jth level, $\hat{d}_{j,k}$ is the thresholded value, and t is the threshold. There are various soft thresholding rules, like fixed threshold ('sqtwolog'), 'rigrsure' based on Stein's unbiased risk estimate, 'heursure' a combination of first two rules, and 'minimax' based on mean square error [17].

The soft thresholding rules were selected for our application, and it is applied in each level (A5, D5, …, D1) for selective truncation of the wavelet coefficients. The thresholded coefficients at different levels are shown in Fig. 2.

c. Reconstruction—After addition of the selected coefficients at each level, the reconstruction was done by the inverse discrete wavelet transform (IDWT).

3 Results and Discussions

For evaluating the denoising performance, the objective assessment was done by computing the following metrics which are common for any denoising operation.

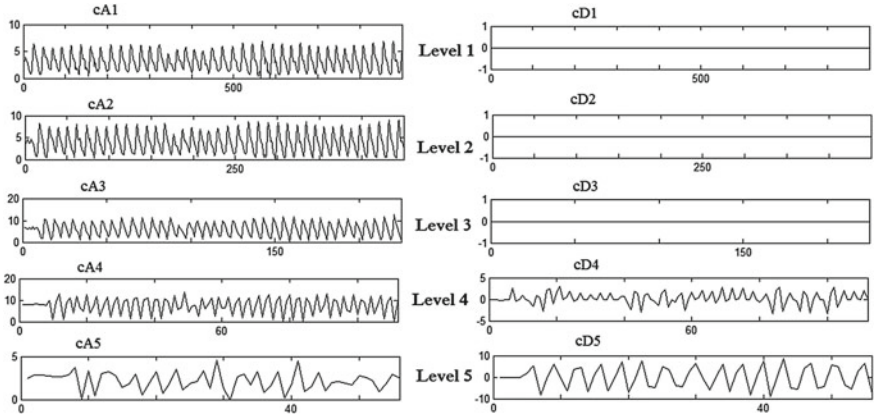

Fig. 2 Soft thresholding applied at different levels using Db6

$$
\begin{aligned}
&MSE\ (Mean\ Square\ Error) = \tfrac{1}{N}\sum_i [x(i) - \tilde{x}(i)]^2 \\
&MAE\ (Maximum\ Absolute\ Error) = \max[x(i) - \tilde{x}(i)] \\
&PNR\ (Percentage\ Noise\ retention) = \tfrac{P_{ds} - P_{cs}}{P_{cs}} \times 100 \\
&SNR_i\ (Signal\ to\ noise\ ratio\ improvement) = 10 \times \log \frac{\sum_i \frac{x^2(i)}{n^2(i)}}{\sum_i \frac{x^2(i)}{[x(i)-\tilde{x}(i)]^2}}
\end{aligned}
\tag{1}
$$

where x = clean signal, $\tilde{x}$ = reconstructed signal, P_{cs} = power of clean signal, N = number of samples, P_{ds} = power of reconstructed signal, n = noisy signal, and P = $10 \times \log\sum|x(i)|^2$. Among these, MSE provides the global error figure, since errors can be positive or negative. PNR provides the residual noise that is retained in the preprocessed signal. SNR_i actually denotes the ratio of input and output SNR (to the preprocessing algorithm), where $x(i)-\tilde{x}(i)$ is the residual noise. MAE is the maximum absolute sample-to-sample error after reconstruction and local residual noise. Table 1 shows these parameters for six arbitrarily chosen healthy volunteers' data for three levels of motion using 'rigrsure' thresholding rule. Among the parameters, we observed that the MAE, averaged over the six volunteers, remains almost unchanged, while MSE and PNR increase slightly with enhanced noise, as expected. Computed over all volunteers' data, for level 1 noise, the average MSE, PNR, MAE, and SNR are 0.104, 2.05, 0.89 mV, and 14.12, respectively. When the noise level increases to level 2, these values are 0.143, 2.44, 0.983 mV, and 11.45, respectively. For highest level 3, these values are 0.230, 2.855, 0.910 mV, and 12.54, respectively. In summary, with noise-level increase, the change in MSE, PNR, MAE, and SNR are 37%, 19%, 10%, and 18%, respectively, from level 1 to 2 and 60%, 16%, 7%, and 9.51%, respectively, for level 2 to level 3. Among these, the MAE is least changed, which means the local distortion could be kept lower in the denoising process.

Table 1 Denoising parameters for db6 mother wavelet function

Volunteers' detail (age, M/F, weight in Kg, height in cm)	Level of noise	MSE	PNR	MAE (mV)	SNR
#1 (27, M, 59, 183)	1st	0.09	1.16	0.92	11.26
	2nd	0.19	2.76	1.12	8.29
	3rd	0.21	3.09	1.01	5.08
#2 (43, M, 72, 173)	1st	0.18	2.85	1.05	7.84
	2nd	0.20	2.98	1.16	7.26
	3rd	0.16	2.24	1.17	7.43
#3 (29, F, 55, 167)	1st	0.23	3.40	1.02	5.06
	2nd	0.30	3.77	1.47	4.33
	3rd	0.43	6.89	0	2.43
#4 (24, M, 65, 167)	1st	0.06	1.83	0.65	15.92
	2nd	0.06	1.71	0.38	14.27
	3rd	0.11	2.77	0.77	10.39
#5 (24, M, 68, 170)	1st	0.14	2.58	1.01	33.07
	2nd	0.10	3.45	0.60	20.54
	3rd	0.11	0.33	1.07	19.33
#6 (24, F, 60, 157)	1st	0.07	0.79	0.97	11.27
	2nd	0.09	0.27	1.19	15.03
	3rd	0.18	1.68	1.44	36.59

The denoising performance is also pictorially represented using Fig. 3 for volunteer 1. The upper panel shows the original and reconstructed signal superimposed, with the residual, i.e., the sample-to-sample error in lowest panel.

Table 2 shows the denoising parameter values for different noise levels using various thresholding rules for volunteer #1 using Db6 wavelet. Here, we studied volunteer 1 data for different levels of noise. It is clearly observable from Table 1 and 2 that MSE value is minimum for 'rigrsure' thresholding rule, while 'heursure' provides the least performance. For local distortion assessment, the fixed thresholding provides worst performance, but its SNR improvement is very good (Fig. 4).

In the next phase, four clinical features: systolic peak height, diastolic peak height, peak-to-peak time, and crest time of the reconstructed data were compared with the original signal to assess the percentage deviation for five volunteers as in Table 1. The used noise levels are level 1 at a proportion of 100 and 200%. The deviations are shown in Fig. 5. It is observed that for volunteer #1, there is no variation of peak-to-peak time event for 200% of noise, while the other features slightly increase. For volunteer #2, the crest time changes by 25% in denoised data. As a general observation, using level 1 noise at 200% proportion, most of the features could be retained within 15% of their original values.

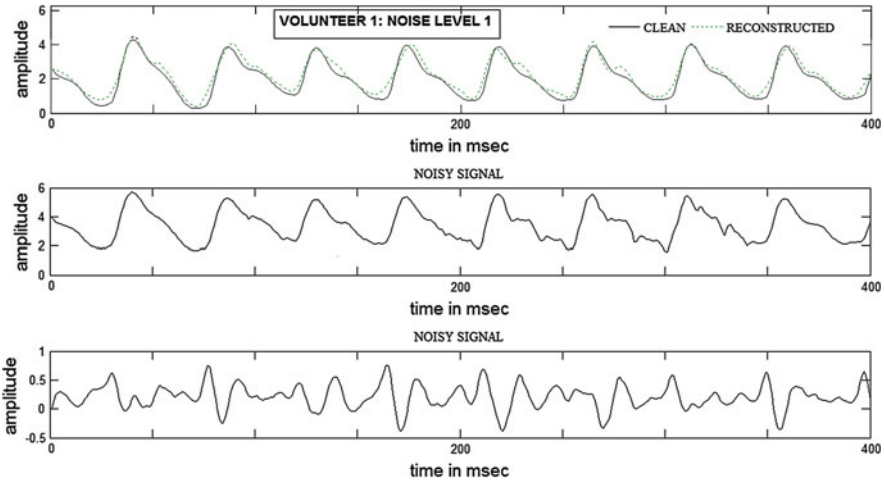

Fig. 3 Subjective assessment of denoising performance

Table 2 Denoising parameters for different thresholding rules (Volunteer #1, Db6)

Level of noise	Threshold rule	MSE	PNR	MAE (mV)	SNR_i
1st	sqtwolog	0.77	2.78	2.21	2.21
	heursure	0.92	2.09	0.92	0.92
	minimax	0.39	1.53	1.53	1.53
2nd	sqtwolog	0.45	0.62	1.77	1.77
	heursure	0.19	2.33	1.12	1.12
	minimax	0.24	0.86	1.19	1.19
3rd	sqtwolog	0.48	1.07	1.50	1.50
	heursure	0.21	2.60	1.02	1.02
	minimax	0.24	1.02	1.21	1.21

Table 3 shows the different denoising parameters for various mother wavelet functions for volunteer #1 and noise level 1. It is observed from Tables 1 and 3 that the denoising parameters show better result for Db6 mother wavelet. In terms of MSE, the Symlets 2, 3, and 4 provide the worst performance. The denoising performance is also graphically shown in Fig. 5. In the published literature using DWT-based PPG denoising [15, 16], no quantitative performance is provided. Only [9] reports SNR of 1.732 dB with horizontal motion of PPG sensor and [11] reports SNR improvement from 0.078 to 0.318 dB. The proposed method achieved an average SNR_i of 7.40 dB.

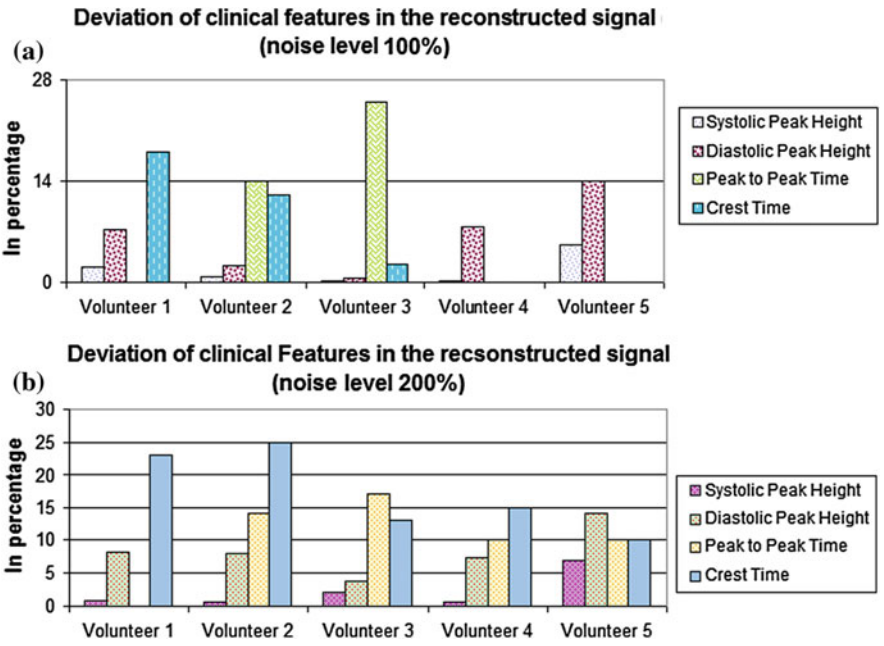

Fig. 4 Deviation of clinical signatures in the reconstructed signal for five volunteers

Table 3 Denoising parameters for different mother wavelet functions (volunteer #1)

Mother wavelets	MSE	PNR	MAE (mV)	SNR_i
Db5	1.27	4.62	2.54	0.25
sym1	3.50	2.10	5.40	7.72
sym2	4.42	0.09	4.59	25.12
sym3	6.10	9.57	4.89	7.58
sym4	2.05	4.76	6.15	11.16
sym5	5.01	4.69	4.60	0.52
coif1	1.17	2.84	3.11	8.82
coif2	2.19	6.50	5.18	11.16
coif3	1.76	4.24	3.43	4.02
coif4	2.37	5.75	4.15	1.98
coif5	2.38	3.41	4.13	3.09

4 Conclusion

In this paper, we present the application of wavelet transform for reduction of motion artifact from PPG signal. Among all wavelets used in the study, the Daubechies wavelet provided best result using 'rigrsure' soft thresholding rule. Using three

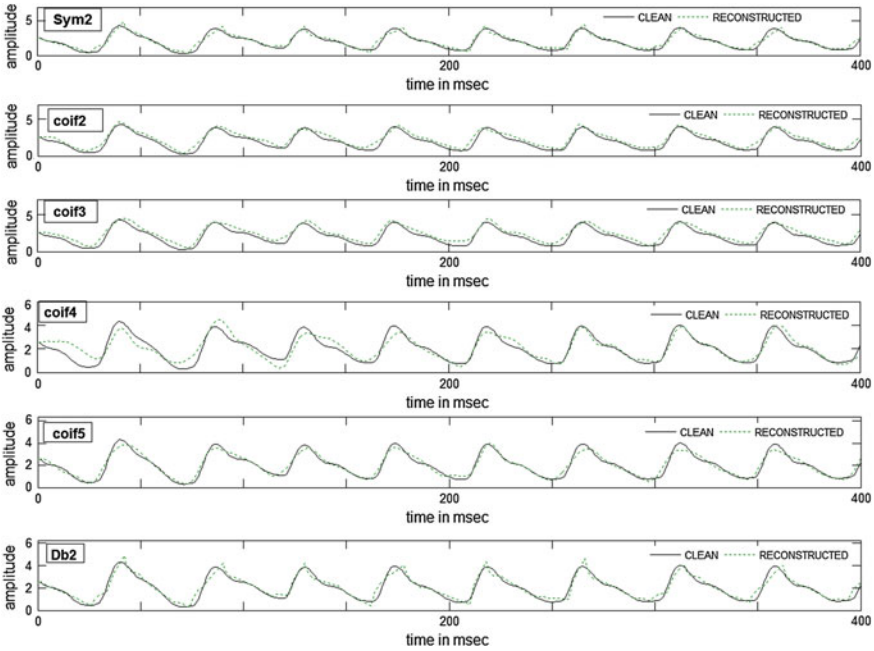

Fig. 5 Denoising performance of different mother wavelet functions

different intensity levels of noise, the reconstructed waveform could retain the most of clinical signatures within 15% of their respective values. We have also made a comparative study between different denoising parameters by using other mother wavelet functions.

References

1. Allen JJ (2007) Photoplethysmography and its application in clinical physiological measurement. Physiol Meas 28(3):1–39
2. Kyriacou PA (2006) Pulse oximetry in the oesophagus. Physiol Meas 27(1):1–35
3. Hertzman AB (1938) The blood supply of various skin areas as estimated by the photoelectric plethysmograph. Am J Physiol 124:328–340
4. Hee X, Goubran RA, Liu XP (2014) Secondary peak detection of PPG signal for continuous cuffless arterial blood pressure measurement. IEEE Trans Instrum Meas 63(6):1431–1439
5. Gil E, Orini M, Bailon R (2010) Photoplethysmography pulse rate variability as a surrogate measurement of heart rate variability during non-stationary conditions. Physiol Meas 31(9):1271–1290
6. Nakajima K, Tamura T, Miike H (1996) Monitoring of heart and respiratory rates by photoplethysmography using a digital filtering technique. Med Eng Phys 18(5):365–372 Elsevier
7. Sweeney KT, Ward TE, MacLoone SF (2012) Artifact removal in physiological signals-practices and possibilities. IEEE Trans Inf Technol Biomed 16(3):488–500

8. Han H, Kim MJ, Kim J (2007) Development of real time motion artifact reduction algorithm for a wearable photoplethysmography. In: IEEE EMBS conference France, pp 1538–1541
9. Raguram M, Madhav KV, Krishna EH, Reddy KN, Reddy KA (2011) On the performance of time varying step–size least mean squares (TVS-LMS) adaptive filter for MA reduction from PPG signals. In: ICCSP Conference, pp 431–435
10. Raguram M, Madhav KV, Krishna EH (2012) A novel approach for motion artifact reduction in PPG signals based on AS-LMS adaptive filter. IEEE Trans Instrum Meas 61(5):1445–1457
11. Castells F, Laguna P, Sornmo L (2007) Principal component analysis in ECG signal processing. Eurasip J Adv Signal Process 2007(1):98–98
12. Cho JM, Sung YK, Shin KW (2012) A preliminary study on photoplethysmogram (PPG) signal analysis for reduction of motion artifact in frequency domain. In: IEEE EMBS conference on IECBES, pp 28–33
13. Wang Q, Yang P (2010) Artifacts reduction based on empirical mode decomposition (EMD) in photoplethysmography for pulse rate detection. In: IEEE EMBC conference, pp 959–962
14. Pinheiro E, Postolache O, Girao P (2012) Empirical mode decomposition and principal component analysis implementation in processing non-invasive cardiovascular signals. Measurement 45(2):175–181. Elsevier
15. Lee CM, Zhang YT (2003) Reduction of motion artifacts from photoplethysmographic recordings using a wavelet denoising approach. In: IEEE EMBS Asian-Pacific conference on biomedical engineering, pp 194–195
16. Raghuram M, Madhav KV, Krishna EH (2010) On the performance of wavelets in reducing motion artifacts from photoplethysmographic signals. In: IEEE international conference on ICBBE, China, pp 121–128
17. Wavelet toolbox user guide MATLAB®. www.mathworks.com